Infrared multiphoton excitation of polyatomic molecules

T. B. Simpson,[a] J. G. Black,[b] I. Burak,[c] E. Yablonovitch,[d] and N. Bloembergen
Gordon McKay Laboratories, Harvard University, Cambridge, Massachusetts 02138

(Received 12 February 1985; accepted 9 April 1985)

We present a systematic study of the infrared multiphoton excitation and dissociation of several polyatomic molecules. The molecules range in size from SO_2, with three vibrational modes, to C_3F_7I, with 27. A gradual transition occurs from intensity dependent excitation, characteristic of a sparse density of vibrational states in small molecules, to a fluence dominated absorption characteristic of a quasicontinuum of vibrational states in large, heavy molecules. Molecules with ten or more atoms showed no intensity dependence under pulsed CO_2 laser excitation at a fixed energy fluence. For a molecule to have a high probability of dissociation under realizable conditions of laser intensity and fluence, quasicontinuum region excitation must dominate. All molecules appeared to have statistically coupled vibrational modes at high levels of vibrational energy.

The infrared multiphoton excitation (IRMPE) and dissociation (IRMPD) of polyatomic molecules have been studied for over a decade.[1] The study of the interaction of an isolated polyatomic molecule, unperturbed by collisions, with intense, high energy laser pulses was motivated by the technological goals of laser isotope enrichment and bond selective chemistry. Molecules ranging in size from triatomics to large molecules have been studied. To date, however, there has been no systematic comparison of molecules of widely varying size and mass under a variety of laser excitation conditions. Such a study is important because the qualitative models[1,2] of IRMPE and IRMPD are built around the overriding importance of the density of infrared active molecular eigenstates in the vicinity of the laser frequency. Further, IRMPD in three- and four-atom molecules had not been unambiguously established.

In this paper we present the results of a systematic investigation of the size dependence of IRMPE and IRMPD in a series of polyatomic molecules. We elaborate and add to our published preliminary data on OCS[3] and SO_2.[4] Unpublished results from Black's thesis[5] on CF_2HCl, CF_3I, CF_3CDCl_2, C_3F_7I, and hexafluoroacetone are presented. Our published data on SF_6,[6] DN_3,[7] and NH_3[8] are briefly summarized and reviewed in the context of the variation of the vibrational density of states with size and mass. IRMPE is shown to be an extremely general phenomenon, but to depend strongly on this density of states. The molecules range in size from SO_2, with three vibrational modes, to C_3F_7I, with 27. At one extreme, excitation of SO_2 is determined by the peak laser intensity. Excitation of C_3F_7I, however, depends on the time integrated intensity, or fluence, of the laser pulse. Molecules of intermediate size show a consistent progression between these two extremes.

Dividing this paper into sections, we first briefly review the model of the IRMPE of polyatomic molecules, pointing out parameters of excitation which will lead to experimentally distinguishable results. Second, the experimental apparatus and procedures are discussed. Tests which show that the excitation occurs under collision free conditions are emphasized. We measure the average number of photons absorbed per molecule $\langle n \rangle$ and the dissociation yield Y_{diss} as a function of CO_2 laser intensity and fluence. This gives us two important pieces of information about the vibrational energy distribution of molecules following IRMPE: the mean of the distribution and the high energy tail. Following the presentation of these results, they are discussed in terms of the model and compared with other experimetnal results.

I. IRMPE MODEL

Three regions of vibrational excitation have been distinguished to describe the IRMPE of polyatomic molecules.[9] The first region has been called the discrete state region because at low levels of internal energy a molecule has states well separated in energy. If one excites molecules prepared in one, or a few, well defined initial rotational vibrational states with monochromatic cw laser radiation of low intensity, the discrete nature of the true molecular eigenstates (ME) will remain apparent even at high levels of vibrational excitation. In IRMPE a high intensity, finite bandwidth laser pulse is used. At a fixed frequency, one has to find excited states, which are connected to the initial state by multiphoton matrix elements with relatively small detuning in the virtual intermediate stages and for which energy can be conserved. This latter condition requires that the excited state lies within a narrow range centered at $nh\nu_L$ above the initial state, where n is the number of laser quanta needed to reach an excitation level and $h\nu_L$ is the laser photon energy. The width of this range is determined by the spectral width of the laser pulse and by the dynamic Stark shifts, which are on the order of the Rabi frequency. In small molecules it will be rare to find discrete states at moderate levels of vibrational excitation for which a multiphoton transition is allowed at a given ν_L. Thus a large fraction of the molecules may remain "bottlenecked" in the initial state.

[a] Present address: Harry Diamond Laboratories, 2800 Powder Mill Road, Adelphi, MD 20783.
[b] Present address: Lincoln Laboratory, Mass. Institute of Technology, P. O. Box 73, Lexington, MA 02173.
[c] Permanent address: Institute of Chemistry, Tel Aviv University, Tel Aviv, Israel.
[d] Present address: Bell Communications Research, Murray Hill, NJ 07974.

 0021-9606/85/140628-13$02.10

For very high excitations in small molecules and lesser excitations in larger molecules, the vibrational molecular eigenstates ME become superpositions of all normal modes. The oscillator strength of the multiphoton transition will be distributed over many ME. The density of accessible states $\rho(\nu)$ grows, reaching the point, where

$$\rho^{-1} < \Delta\nu_L/c. \tag{1}$$

Here, ρ is the density of states per wave number accessible by the absorption of a photon, $\Delta\nu_L$ is the frequency spread of the laser pulse Fourier components, and c is the speed of light. For pulsed excitation $\Delta\nu_L \gtrsim (2\pi t_p)^{-1}$, where t_p is the laser pulse duration. When inequality (1) is satisfied the accessible states form a quasicontinuum insuring that resonant, stepwise one-photon excitation is possible. The transition from the discrete state to the quasicontinuum region occurs at a level of vibrational excitation, which depends not only on the molecular species but also on the parameters of the exciting laser pulse.

In the quasicontinuum, interest is focused on the large number of ME in each interval $nh\nu_L \pm h\Delta\nu_L$. The congestion produced by the large numbers of initial and final states involved leads to the description of the IRMPE process in terms of phenomenological rate equations

$$\begin{aligned} dX_n/dt = &-(\sigma_{n,n+1} + \sigma_{n,n-1})(I/h\nu_L)X_n \\ &+ \sigma_{n-1}(I/h\nu_L)X_{n-1} \\ &+ \sigma_{n+1,n}(I/h\nu_L)X_{n+1} - k_{n>M}X_n\,. \end{aligned} \tag{2}$$

In Eq. (2) X_n is the population fraction of molecules absorbing n photons, $\sigma_{n,m}$ is the cross section for laser pumping from level n to level m, I is the laser intensity, $h\nu_L$ is laser photon energy, and $k_{n>M}$ is the dissociation rate for molecules excited above level M. Ignoring the dissociation term the parameter of excitation becomes $Idt = dJ$, where J is the laser fluence.

The use of rate equations is justified when the excitation process can be described by first-order time dependent perturbation theory and the assumptions underlying Fermi's Golden Rule are valid. The frequency spread of transition oscillator strength Γ, the nature of the laser coupling, and the density of accessible states ρ must be considered. With these parameters in mind the first requirement for validity of the rate equations (2) is

$$h^{-1}\langle(U)\rangle E_L \ll \Gamma. \tag{3}$$

Here $\langle(U)\rangle$ is the dipole matrix element of the vibrational mode resonant with the laser and E_L is the laser electric field strength. This inequality states that the interaction of normal mode states due to the anharmonic coupling is much stronger than the laser-molecule interaction. Between each absorption event the molecule will relax out of the laser prepared normal mode configuration and lose coherence with the laser field. There are a few specific cases, in which rate equations may be applied, even if Eq. (3) is not satisfied.[10]

To make the connection with Fermi's Golden Rule we must make a transformation from the normal mode picture to the molecular eigenstate description. The dipole strength is distributed among the eigenstates. However, the following sum rule must hold[11]:

$$\langle(u)\rangle^2 = \langle(U)\rangle^2 c/\Gamma\rho, \tag{4}$$

where $\langle(u)\rangle$ is an average ME dipole matrix element. The quantity $\Gamma\rho$ is simply the number of states into which the zero-order strength is diluted.

The inequalities for the applicability of Fermi's Golden Rule can be summarized:

$$\rho^{-1} \ll \Delta\nu_L/c, \quad \frac{\langle(u)\rangle E_L}{hc} \ll \Gamma/c, \tag{5}$$

where the comma is to indicate that some care must be taken when considering the two laser coupling terms.[11] When the number of states that can be coupled through the laser bandwidth is much greater than through intensity induced dynamic Stark shifts then the rate equation description (2) applies. However, when the stepwise Rabi frequency dominates, the possibility of a coherent multiphoton transition must also be considered. For the rate equations to apply the random coupling hypothesis[12] must also be invoked. Satisfying inequality (5) with $\Delta\nu_L$ ensures the applicability of the rate equation description throughout the laser pulse, not only during times of high laser intensity.

Finally, a third region of a true continuum begins when the bandwidth of the accessible ME's causes states to overlap. For the polyatomics discussed here this will generally occur above the dissociation limit where the states are lifetime broadened. Dissociation accounts for the loss mechanism in the rate equations.

The density of accessible molecular eigenstates is a central parameter in the description of the IRMPE of polyatomic molecules. Due to the anharmonic coupling of the vibrational modes, excitation is not limited to a single ladder of states associated with a resonant vibrational oscillator. As the molecule absorbs energy, vibrational selection rules can be expected to break down and the density of states accessible through infrared excitation will increase dramatically. An estimate of the density of accessible states can be made by calculating the vibrational state density. Figure 1 plots a

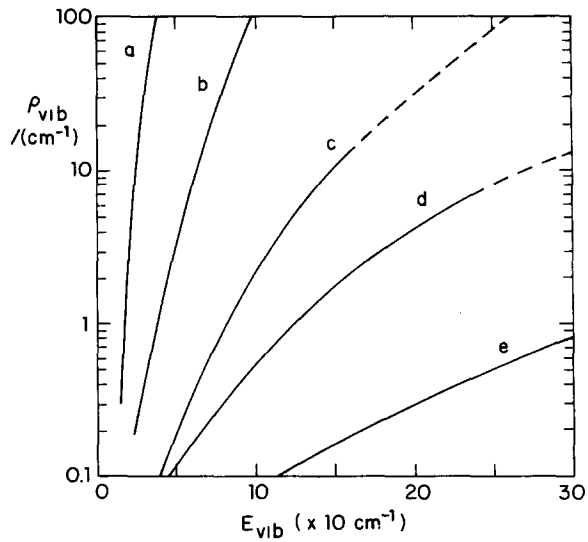

FIG. 1. Whitten–Rabinovitch calculation of the density of vibrational states as a function of vibrational energy for several of the molecules discussed in this work. (a) SF_6, (b) CF_2HCl, (c) DN_3, (d) OCS, (e) SO_2.

Whitten–Rabinovitch type calculation[13] of the vibrational state density for several of the molecules discussed in this work. This estimate should be considered as a relative measure of the growth of the density of accessible states. For instance, a breakdown of rotational selection rules leading to a total rotational-vibrational coupling would increase the density of accessible states by roughly two orders of magnitude. The Whitten–Rabinovitch calculation only provides an estimate of ρ in the eigenstate picture. In the normal mode description the density of states must saturate as has been discussed by Stone *et al.*[14,15] For comparison, our CO_2 laser will have a bandwidth between 10^{-3} and 10^{-1} cm^{-1} depending on which pulse type is used.

Each of the three regions has distinguishable parameters. IRMPE through the region of discrete states depends on the peak laser intensity. In the quasicontinuum region laser fluence controls the excitation. Finally, in the continuum IRMPD becomes possible.

II. EXPERIMENTAL APPARATUS AND PROCEDURES

The pulsed CO_2 laser has been designed to produce four types of laser pulses with energy up to 1 J; 100 ns multimode, 100 ns single mode, 20–40 ns, and 0.5 ns.[16] The laser beam is brought to a focus by various combinations of mirrors and lenses depending on the size of the beam waist desired. To correct for fluctuations, laser energy is monitored for each shot by a pyroelectric detector. Absolute calibration of the CO_2 laser pulse energy is made with a calorimeter. For the purposes of these experiments, the laser transverse intensity (or energy) profile must be well known. An accurate determination of the beam is demanded for calculation of the fluence of each shot. The beam measurements are performed by translating a pyroelectric detector, which is masked by a 50 μ pinhole, across the beam at the measurement location both horizontally and vertically. The results are fitted to a Gaussian profile with good agreement. Error in the absolute calibration of beam fluence is about 30%.

Measurements were made on room temperature gas samples contained in aluminum cells fitted with salt windows at each end. The inner diameter of the aluminum cell is 2 cm. Either a side window with photomultiplier tube or a microphone for optoacoustic measurements could be fitted. The gases used in this work were obtained commercially and used without further purification. Gas pressures were measured by a capacitance manometer. Absolute pressure accuracy is $\pm$ 2 mTorr.

Data collection and storage is carried out with a DEC LSI-11 based data acquisition system.[17] There are several data channels with sample and hold amplifiers that are used to store signals from the pyroelectric detectors, microphone, photodiode, or integrated photomultiplier signals. If the temporal characteristics of a signal, generally a photomultiplier signal, need to be measured then such a signal is digitized on a Biomation Model 8100 waveform recorder.

Our desire to determine the energy absorbed by molecules under collisionless conditions and uniform light beam characteristics points to the use of optoacoustic (sometimes called photoacoustic, to avoid confusion with acoustooptic) calorimetry. One must focus the laser beam to attain the intensity and fluences required to induce multiphoton absorption. This focusing results in the beam being reasonably uniform only over a restricted length. We have thus circumscribed the problem to that of measuring a low pressure sample of limited length, i.e., optically thin. A direct transmission measurement of absorption in such a sample is difficult, so we must employ a zero background technique, optoacoustic calorimetry. All other parameters being equal, a transmission measurement of absorption cross sections is at best 37% as sensitive as a null approach, and for optically thin samples the difference is much more pronounced.[5]

The main requirement we place upon the optoacoustic technique is that it shall represent a linear measurement of the energy deposited in the cell. Physically this requirement is that the heat generated by the collisional deexcitation of vibrational energy represents a small perturbation to the gas in the cell as a whole. It is this consideration which governs the radius at which the microphone diaphragm is placed. A strong absorption case, such as SF_6, requires that one place the microphone at the periphery of the cell, while for more weakly absorbing molecules, the microphone is moved closer to the beam for more sensitivity.

The energy deposition measurements are relative in nature and must be absolutely calibrated by a transmission measurement. For the strong absorbers, the cell is made optically thick by filling it with 5 Torr of the studied sample. The 0.5 ns pulses are used to assure collisionless conditions. These transmission measurements are easily performed using a calorimeter to compare transmission with the cell full and evacuated. The ratio of the two ratios of calorimeter to reference arm gives the transmission, which is easily analyzed to yield a value for the photons absorbed per molecule at the fixed fluence at which the measurement is taken. With the weaker absorbers, a small amount of SF_6 is added to increase absorption without changing the acoustic properties of the sample. SF_6 has been well studied and the microphone signal from a pure sample of the weak absorber is calibrated against the signal from the mixture.[3]

Since the microphone is only sensitive to the added translational energy of the molecular ensemble, the energy which goes into bond breaking is not measured. If most of the absorbed energy from the CO_2 laser is used to excite molecules over the dissociation threshold where they rapidly fall apart, then the microphone signal is not a good measure of the energy deposited in the system. This behavior is strongly borne out by experiments on SO_2.[4] Another potential complication arises from the possibility of exothermic chemistry following IRMPD. Dissociation products can be quite reactive. The molecules studied here, however, are stable against reaction with their dissociation products, at least on the time scale of interest to the microphone measurement.

For most of the molecules the dissociation yield of unimolecular reactions after multiphoton energy deposition has been measured by the static cell irradiation approach. In brief, we measure the small-signal transmission of a gas sample, irradiate it with a number of pulses of collimated light, and measure the transmission again. The depletion of the molecules in the sample is accompanied by an increase in the transmission. This technique has the advantage of being sim-

ple, generally applicable, and very readily calibrated absolutely. It may be subject to possible secondary reactions or reverse reactions,[18] but these are generally not a problem.

In the static cell measurements, the cell is filled and closed off from the vacuum manifold system, then irradiated by a certain number of pulses. The data acquisition system keeps track of the fluctuations in laser energy, since it is desired that these measurements be taken at constant fluence. Of course, the reference arm is calibrated to determine the exact value of the laser energy, and the average value of the laser energy is taken for the dissociation runs.

It is crucial that collisions play a negligible role in the excitation and dissociation process. The gas-kinetic collision time for polyatomics in the size range of interest is greater than 25 ns Torr.[19] Thus to achieve collisionless absorption conditions we use combinations of gas pressure and laser pulse durations $\leqslant 10$ ns Torr for our measurements. Recent experimental results on SF_6 indicate a very fast, 2 ns Torr, collisional relaxation process for molecules excited into the quasicontinuum.[20] A comparison of our previously published static cell results[6] with those done under collision-free molecular beam conditions[21] shows that this fast relaxation process does not significantly modify the results. At most the long-range collisions, which do not appear to involve significant energy transfer and require a high density of states, may lead to slightly enhanced absorption in the quasicontinuum. Collisions following the laser pulse, but before dissociation, could also influence the IRMPD results. However, calculations indicate that the fraction of molecules excited to states with such long dissociative lifetimes is not large enough to be of significance.[22]

For the three- and four-atom molecules, the fraction of dissociated molecules is too small to be observed through depletion measurements. Instead, IRMPD is detected by introducing a scavenger molecule which reacts with a dissociation product to produce an excited fluorescing molecule. Evaluation of the dissociation yields is carried out by measuring the intensity of the fluorescence signal.

In the case of SO_2, the molecule undergoes dissociation into SO and atomic oxygen. In the presence of NO the following three-body recombination process takes place:

$$O + 2NO \xrightarrow{k_0} NO_2^* + NO.$$

NO_2^* is a molecule formed in a highly excited vibronic level of the ground electronic state. Those states are slightly admixed with vibronic states of excited electronic levels. They therefore possess oscillator strength for optical emission in the visible. Since the emission of NO_2^* is shifted further to the red than the SO_2^* fluorescence, the emissions from the two species are well separated.

The time evolution of the excited NO_2^* molecules is described by the following rate equations:

$$\frac{d[O]}{dt} = -k_0[O][NO]^2, \tag{6}$$

$$\frac{d[NO_2^*]}{dt} = -k_{\text{rad}}^{NO_2}[NO_2^*] - k_1[NO][NO_2^*] + k_0[O][NO]^2, \tag{7}$$

where $k_{\text{rad}}^{NO_2}$ is the average radiative lifetime of excited NO_2 and k_1 is the collisional quenching rate. All experiments were conducted using mixtures with a high $[NO]/[SO_2]$ ratio. This permits us to ignore three-body recombination terms involving SO_2 as well as collisional quenching of the NO_2^* by SO_2. Integration of Eqs. (6) and (7) yields

$$[O] = [O]_0 \exp(-k_0[NO]^2 t) \tag{8}$$

and in the limit $k_0[NO] \ll k_1$ and $k_{\text{rad}}^{NO_2} \ll k_1[NO]$,

$$[NO_2^*] = (k_0/k_1)[NO][O]_0 \exp(-k_0[NO]^2 t). \tag{9}$$

Here, $[O]_0$ is the initial concentration of oxygen atoms. Collision-free dissociation of the SO_2 requires that the amplitude of the chemiluminescence signal be proportional to the [NO] and to the $[SO_2]$ density and that the exponential decay of the signal be inversely proportional to the square of the [NO] density. This is confirmed in Figs. 2 and 3, establishing the collision-free nature of the excitation.

The number of dissociated SO_2 molecules N_{diss} is

$$N_{\text{diss}} = [O]_0 V_{\text{eff}}. \tag{10}$$

The focal volume V_{eff} is

$$V_{\text{eff}} = \pi W_0^2 z_0/2, \tag{11}$$

where W_0 is the beam waist and z_0 is the confocal beam parameter. One can estimate N_{diss} from the initial amplitude of the chemiluminescence I_{chem}:

$$I_{\text{chem}} = A k_{\text{rad}}^{NO_2}(k_0/k_1) N_{\text{diss}}[NO]. \tag{12}$$

Here, A is a factor involving the spectral and electrical characteristics of the PMT and the solid angle viewed. A value of 50 μs has been used for the average radiative lifetime of NO_2^*[23] and a value of 2×10^6 s^{-1} Torr^{-1} has been used for k_1.[23] The three-body rate $k_0 = 1.3\times10^2$ s^{-1} Torr^{-2} can be calculated from Fig. 3. The dissociation yield Y_{diss} is the

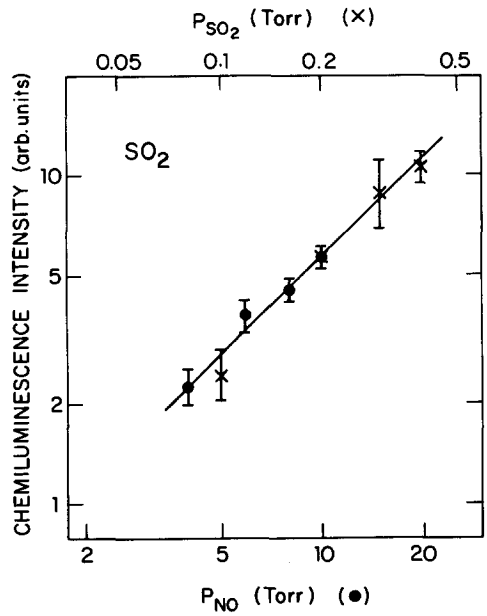

FIG. 2. Log–log plot of the intensity of three body chemiluminescence following IRMPD of SO_2 plotted as a function of SO_2 partial pressure (×) and NO pressure (●). The CO_2 laser with 0.5 ns pulses is tuned to R (22) line in the 9.4 μm branch.

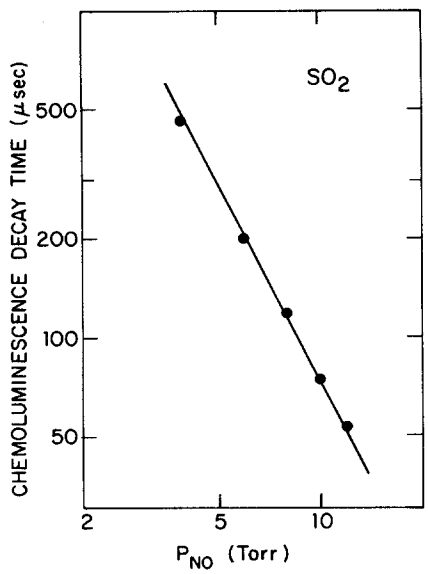

FIG. 3. Log–log plot of the three body chemiluminescence decay time following IRMPD of SO_2 plotted as a function of NO pressure. The line is proportional to p^{-2}. Laser conditions are the same as Fig. 2.

ratio of N_{diss} to the number of SO_2 molecules in the focal volume. This calibration is subject to some error, and thus is not meant to be of high precision. For instance, the PMT response is not constant over the broad emission spectra of the emitting species. Estimates must be made of the fraction of the emission that falls outside of the spectral range of sensitivity of the PMT. Accuracy is estimated to be within a factor of 3. Such accuracy is good enough to provide important information about IRMPD in weakly absorbing molecules.

Another technique utilizing chemical scavengers was necessary to measure IRMPD in OCS. Previously, we reported no evidence of dissociation using the static cell irradiation approach.[3] As stated above, there was no fluorescence from OCS and NO mixtures. However, OCS is expected to dissociate into CO and S, not CS and O.

If the OCS is mixed with NO_2, which does not absorb, then the following chemistry will occur if the OCS undergoes IRMPD:

$$S + NO_2 \rightarrow SO + NO + 2\ eV, \quad (13)$$

$$SO + NO_2 \rightarrow SO_2 + 2.5\ eV. \quad (14)$$

These two reactions have rates[24] faster than $10^6\ s^{-1}\ Torr^{-1}$ and lead to an increase in the translational energy of the system equivalent to approximately 35 CO_2 laser photons per dissociated molecule. Reactions involving NO and CO will proceed more slowly.

The following procedure was used. The average number of photons absorbed per molecule $\langle n \rangle$ in pure OCS gas was measured, calibrated by the previously described technique, and compared with the acoustic signal from a mixture of OCS and NO_2. There will be an excess signal from the chemistry following dissociation. Dividing the excess by 35 gives the yield of dissociated molecules. Due to the small signal changes inherent in this technique there could be no rigorous test to show collision-free excitation. However, this experiment was run under conditions where the optical tests showed collision-free excitation for other small molecules.

III. EXPERIMENTAL RESULTS

A. Triatomic molecules

The molecule SO_2 is at the limit of small polyatomic molecules, having only three normal mode frequencies. The normal mode most nearly resonant with the CO_2 laser transitions is the ν_1 stretch centered at 1150 cm^{-1}. This is 70 cm^{-1} higher in energy than the strong lines of the R branch of the 9.4 μ laser transition. The ν_1 stretch is down shifted by 5–10 cm^{-1} with each quantum for the first few transitions.[25] In spite of the large detuning, IRMPE of SO_2 is observed though the mean excitation energy is small. Figure 4 plots $\langle n \rangle$ as a function of laser intensity I for 0.5 ns pulses with the CO_2 laser tuned to the R (22) line of the 9.4 μ branch. For comparison, 300 GW/cm^2 corresponds to 200 J/cm^2.

As we have previously reported IRMPE only takes place on the R branch, 9.4 μ transition lines of the CO_2 laser. At the highest laser intensity most molecules still remain bottlenecked in the ground state, and all of the acoustic signal is accounted for by a small fraction of molecules excited to high vibrational energy states.[4] These states emit UV fluorescence due to the mixing of excited vibronic levels of the ground electronic state with electronically excited manifolds. The yield of molecules excited to the fluorescing levels has been determined[4] as a function of the CO_2 laser intensity. A comparison between the excitation yields and the corresponding values of photons absorbed per molecule $\langle n \rangle$ indicates that lower vibrational levels of SO_2 are not populated. The IRMPD process involves a direct absorption of at least 25 photons exciting the ground vibronic state to the region of fluorescing levels. Since the process is enhanced by near resonances the excitation yield varies with the laser intensity I as I^β where $\beta \ll 25$.

The dissociation yield can be estimated through the re-

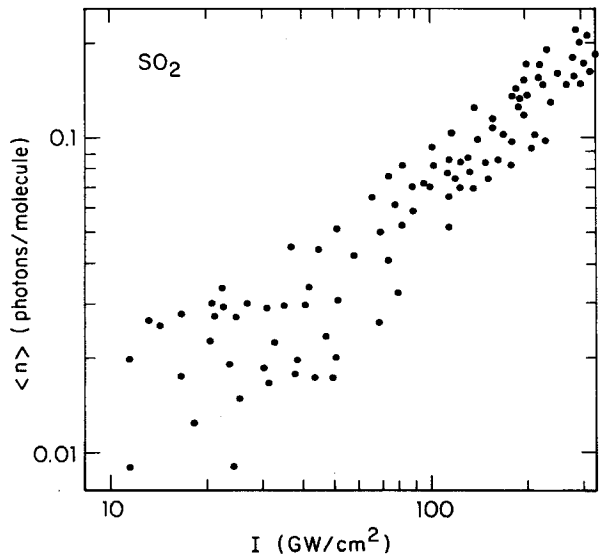

FIG. 4. Log–log plot of the average number of photons absorbed per molecule $\langle n \rangle$ in SO_2 plotted as a function of CO_2 laser intensity. The laser with 0.5 ns pulses, is tuned to R (22) in the 9.4 μm branch. Each data point is an average of two shots.

combination fluorescence from SO_2 and NO mixtures discussed above. Figure 5 plots the dissociation yield as a function of intensity. Again, the laser line is the R (22) transition of the 9.4 μ branch. This is the first unambiguous evidence for IRMPD in a triatomic molecule.

Over the intensity range of Fig. 5 the dissociation yield is comparable to the yield of SO_2 molecules excited to high vibrational states previously reported.[4] It takes approximately 30 IR photons to reach the fluorescing SO_2 states and 42 to reach the dissociation threshold. Therefore, it appears to be relatively easy for the highly excited molecule to absorb additional IR photons. This is confirmed by recent experiments on IRMPD of SO_2 molecules initially prepared by a UV laser.[26] In that case, significant IRMPE was possible at a CO_2 laser intensity and fluence orders of magnitude lower than was necessary for the room temperature ensemble used here.

The optoacoustic measurements on OCS are summarized in Fig. 6. The CO_2 laser was tuned to the P (24) line of the 9.4 μ branch which is resonant with the $2\nu_2$ absorption overtone feature. Due to the fact that gas pressures above 2 Torr were necessary for a measurable signal, only the 0.5 ns pulses could be used. Dissociation yields were also quite small. They were measured using the increased optoacoustic signal from OCS and NO_2 mixtures discussed above. With this technique, dissociation yields $<10^{-3}$ at 50 J/cm^2 and $6(\pm 4)\times 10^{-3}$ at 200 J/cm^2 were measured.

In contrast to SO_2 and OCS no evidence of IRMPE and IRMPD of NO_2 was observed at CO_2 laser intensities and fluences to 300 GW/cm^2 and 200 J/cm^2, respectively. Like SO_2, NO_2 excited to high vibrational states can fluoresce and NO_2 and NO mixtures will yield chemiluminescence following three-body reactions. No light emission was observed. Given that the nearest vibrational modes of NO_2 are detuned by approximately 200 cm^{-1} from the CO_2 laser transition, these results are not surprising. If NO_2 is initially excited to high vibrational states by a visible laser pulse, then significant IRMPE and IRMPD are possible.[27]

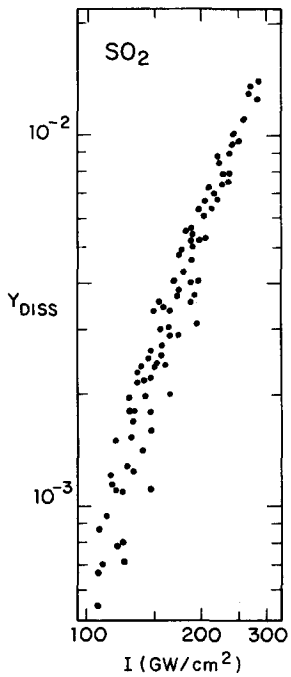

FIG. 5. Log-log plot of the dissociation yield of SO_2 molecules Y_{diss} plotted as a function of laser intensity. Data points are the calibrated three body chemiluminescence signal. The CO_2 laser with 0.5 ns pulses, is tuned to R (22) in the 9.4 μm branch. Each point is one laser shot.

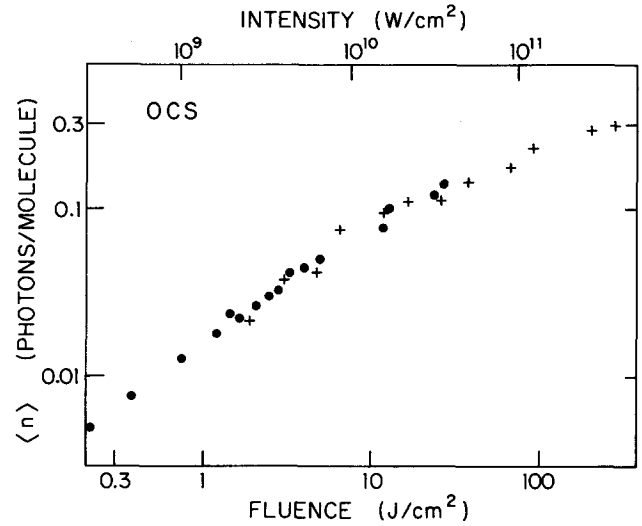

FIG. 6. Log-log plot of the average number of photons absorbed per molecule $\langle n\rangle$ in OCS plotted as a function of laser intensity and fluence. The 0.5 ns laser pulses are tuned to P (24) in the 9.4 μm branch. (○) are data with less tightly focused laser than (+).

B. Four-atom molecules

Recently, we published results on the IRMPE and IRMPD of NH_3.[8] The IRMPD measurements used fluorescence from HNO* molecules formed from the three-body reaction of the atomic hydrogen dissociation product of NH_3 with two NO molecules.[28] The kinetic analysis is similar to that for SO_2 dissociation discussed in Sec. II and collision-free dissociation is observed.[29]

The most interesting feature of these results is that the dissociation yield measurements do not correlate with the optoacoustic measurements of average excitation. The dissociation measurements show a smooth trend toward larger signals as the excitation wavelength is increased while the energy deposition measurements show a more random behavior. The anomalous optoacoustic results indicate that some fortuitous resonances to states at a few photons of vibrational energy can have a major influence on the number of photons absorbed. These exact n photon resonances are not necessary, however, for excitation up to the dissociation limit. In fact, it is not clear that a small number of exact resonances greatly aides IRMPE to highly excited states in NH_3.

Another four-atom molecule that we have studied is DN_3.[7] For a given internal energy it has a vibrational density of states an order of magnitude larger than that of NH_3. When the average number of photons absorbed and the dissociation yield are plotted as a function of laser fluence, a strong pulse duration, i.e., intensity, dependence is evident.[7] Rather than simply reproduce our previous data here, we choose to plot in Fig. 7 the dissociation data as a function of the average number of photons absorbed. The two pulse lengths used, 0.5 and 30 ns, give similar data when plotted

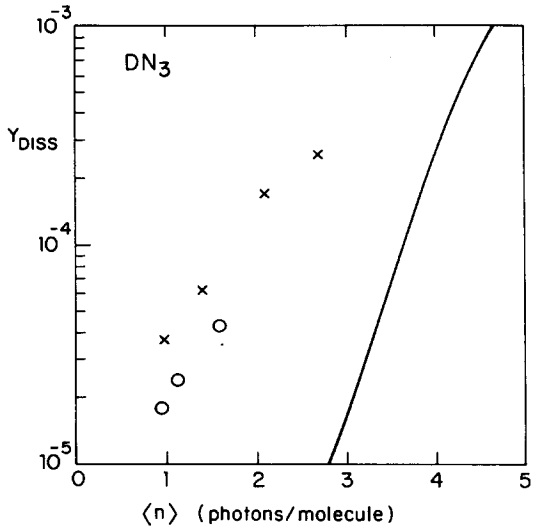

FIG. 7. Semilog plot of the dissociation yield Y_{diss} as a function of the average number of photons absorbed per molecule in DN_3. (×) 0.5 ns pulses. (○) 30 ns pulses. The CO_2 laser is tuned to $P(18)$ in the 10.6 μm branch. The experimental points are taken from Ref. 7. The solid line is calculated on the assumption of a thermal distribution at an energy corresponding to $\langle n \rangle$.

this way. For a given level of excitation the final distribution of excited states, measured by comparing the mean and high energy tail, appears to be relatively insensitive to pulse duration.

Also shown in Fig. 7 is a curve giving the dissociation yield assuming a Boltzmann distribution of the moleculear ensemble. For DN_3 and larger molecules this curve gives the expected fraction of molecules excited above the dissociation threshold for a Boltzmann distribution corresponding to an average energy given by $\langle n \rangle$ plus the vibrational energy at room temperature. The Whitten–Rabinovitch aproximation is used to calculate the density of states and the QRRK unimolecular reaction theory is applied.[22] In Fig. 7 the experimental data points lie to the left of the thermal curve indicating a broader than thermal distribution for DN_3 following IRMPE.

Our measurements do not allow a definitive statement as to whether the fraction of excited three- and four-atom molecules comes from a small fraction of the initially populated rotational levels or are representative of the whole ensemble. Molecules that start in certain rotational states could have preferential absorption pathways. However, at the very high laser intensities used to excite the small molecules the transition Rabi frequency is on the order of 10 cm^{-1}, wide enough to overcome the initial detuning of the first photon transition for most of the OCS and DN_3 population. Further, the anharmonicity of small molecules like OCS and SO_2 is also approximately 10 cm^{-1} per vibrational quantum. While specific pathways for some rotational states could be more resonant over some range of excitation, it is unlikely that the OCS and DN_3 molecules that reach high levels of excitation have had some preferential excitation pathway due to an initial rotational state. In SO_2, the CO_2 laser frequency is sufficiently nonresonant that the excited fraction of molecules may come from the high energy tail of the initial rotational distribution. However, even here, the large anharmonicity works to bring the more populated rotational states into resonance at the 4–6 vibrational quanta level.

C. Larger molecules

Continuing to increase the size of molecule studied we move on to CF_2HCl. The optoacoustic data are presented in Fig. 8. The absorption is much stronger in this molecule allowing data to be taken at 0.1 Torr. Three different pulse types are presented, 0.5 and 100 ns multimode and 100 ns single mode. The multimode pulses have a larger bandwidth and exhibit intensity spikes relative to the temporally smooth single mode pulses. These data were taken at 1086 cm^{-1}, at the "blue" limit of the CO_2 laser. Each point shown in the figure is an average of 15 to 20 experimental data points.

The dissociation data are plotted in Fig. 9. The single mode and multimode data of King and Stephenson[30] permit a direct comparison with our optoacoustic data. The dissociaiton yields corresponding to the single and multimode pulses are plotted vs $\langle n \rangle$, the average number of photons absorbed per molecule. As in the case of DN_3, despite the strong dependence of the dissociation yields on the pulse mode, the two curves nearly coincide, as shown in Fig. 9. As a reference the recent data of King and Stephenson[31] for 2 ns pulses compare well with our 0.5 ns optoacoustic data. These results prove that the enhanced dissociation for increased intensity is due to the increased amount of energy allowed into the molecule, but that the two excitation conditions produce similar distribution widths for constant energies.

A molecule superficially similar to CF_2HCl is CF_3I. Both are substituted methanes. However, the density of vibrational states in CF_3I is much higher and the absorption characteristics are quite different. This molecule has a strong absorption feature at approximately 1075 cm^{-1}, within the tuning range of our laser system. To study the absorption of CF_3I, the laser was tuned to the line at 1074.65 cm^{-1}. The raw optoacoustic data are shown in Fig. 10. Again, as with CF_2HCl, we have three sets of data, corresponding to the

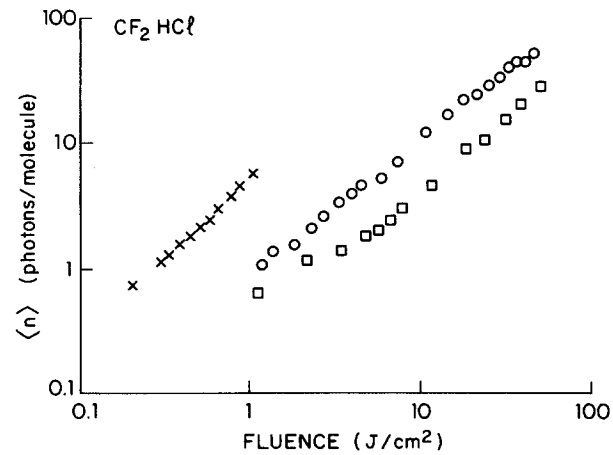

FIG. 8. Log–log plot of the average number of photons absorbed per molecule $\langle n \rangle$ in CF_2HCl as a function of CO_2 laser fluence for three pulse types. The laser is tuned to 1086 cm^{-1}. (×) 0.5 ns. (○) 100 ns multimode. (□) 100 ns single mode.

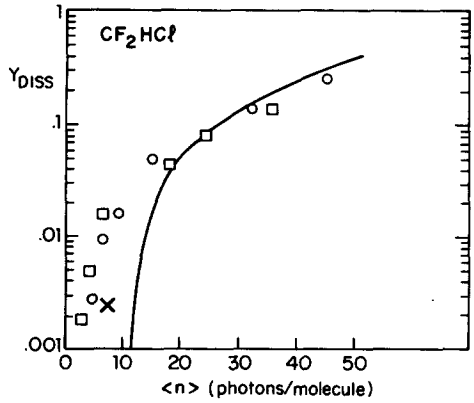

FIG. 9. Semilog plot of the dissociation yield Y_{diss} as a function of the average number of photons absorbed per molecule $\langle n \rangle$ in CF_2HCl. (□) 100 ns single mode. (○) 100 ns multimode. (×) 0.5 ns. The data are obtained by combining our optoacoustic data with dissociation measurements in Refs. 30 and 31. The solid line is the calculated yield on the assumption of a thermal distribution at an energy corresponding to $\langle n \rangle$.

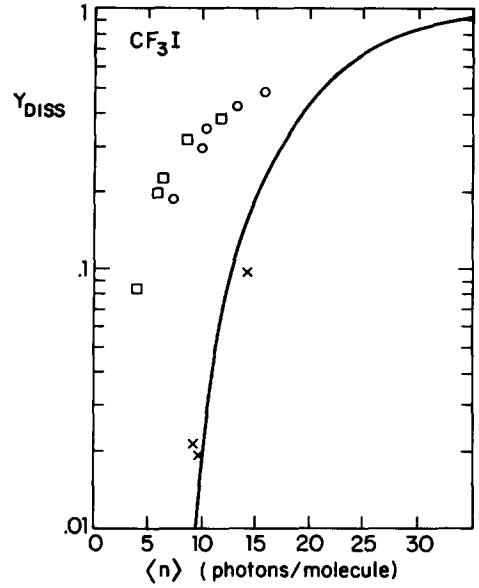

FIG. 11. Semilog plot of the dissociation yield Y_{diss} as a function of the average number of photons absorbed per molecule $\langle n \rangle$ in CF_3I. (□) 100 ns single mode. (○) 100 ns multimode. (×) 0.5 ns. Also shown is the yield assuming a thermal distribution at an energy corresponding to $\langle n \rangle$.

three laser pulse types. Each point shown is an average of 15 to 20 experimental data points.

Our dissociation measurement results are plotted in Fig. 11. Our multimode data are quantitatively consistent with the results of Rossi *et al.*,[32] who employed molecular beam techniques rather than our static-cell method. Their laser excitation conditions are similar to ours. Again, the 100 ns multimode and 100 ns single mode results, which are distinctly different when plotted vs fluence, coalesce when plotted as yield vs average internal energy. The relation of this data to the thermal curve with $M = 20$,[33] is similar to the relation of the 100 ns CF_2HCl data to the thermal curve in Fig. 9.

The seven atom molecule SF_6 has been discussed extensively.[6] We summarize the data in Fig. 12. Note the steady progression to the weakening of the influence of peak laser intensity in this molecule relative to smaller molecules.

In contrast to the situation with three- and four-atom molecules, a large fraction of the CF_2HCl, CF_3I, and SF_6 ensembles can undergo IRMPD at moderate laser intensity and fluence. At these laser intensities the Rabi frequency for a one-photon transition is significantly less than the spread of transition frequencies due to the initial room temperature rotational distribution. Apatin *et al.* have recently shown that the probability of depopulating a rotational state in SF_6 is relatively insensitive to the initial detuning of that state's one-photon transition frequency from the laser frequency.[34] The bottleneck fraction does not come from a subset of the initially populated rotational states but represents the difficulty of depopulating any rotational level when discrete state effects influence the excitation. However, the efficiency of IRMPE of the SF_6 ensemble is increased as the initial rotational and vibrational temperatures are increased.[35] Spectroscopic details play a less important role in determining

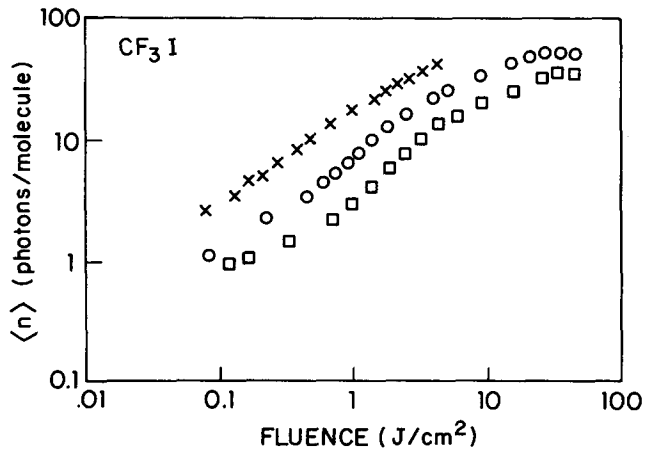

FIG. 10. Log–log plot of the average number of photons absorbed per molecule $\langle n \rangle$ in CF_3I as a function of CO_2 laser fluence for three different pulse types. Laser is tuned to 1075 cm^{-1}. (×) 0.5 ns. (○) 100 ns multimode. (□) 100 ns single mode.

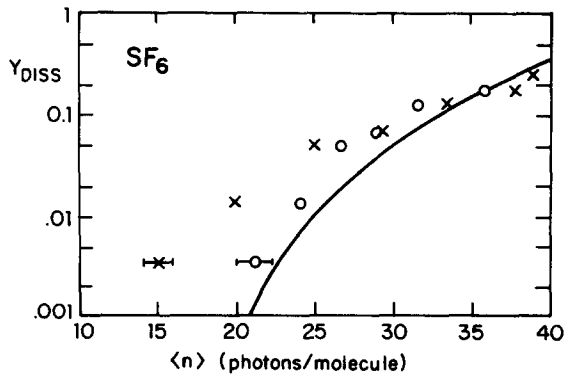

FIG. 12. Semilog plot of the dissociation yield Y_{diss} as a function of the average number of photons absorbed per molecule $\langle n \rangle$ in SF_6. (○) 100 ns, single and multimode. (×) 0.5 ns. Data points are taken from Ref. 3. The solid line to the yield calculated with the assumption of a thermal distribution at an energy corresponding to $\langle n \rangle$.

IRMPE in these molecules than does the energy content of the molecule.

The eight-atom molecule d-Freon-123 (CF_3CDCl_2) drew great attention due to the work of Marling and Herman[36] showing its possible use as a deuterium separation vehicle. It is excellent for this purpose due to the large isotope shift when D is substituted for H. The D isotope which we used was prepared by stirring the commercially available H isotope in a large amount of D_2O, with NaOH added to facilitate the H–D exchange. Due to the preponderance of deuterons in the exchange bottle, eventually the Freon becomes about 98% deuterated, basically a function of the dilution ratio in the bottle.

The excitation frequency used for d-Freon-123 was 936.8 cm^{-1}. The optoacoustic data are plotted in Fig. 13. The data saturates upon absorption of enough photons for extensive dissociation to occur. There is a barely discernible intensity dependence of absorption, but this is less than the relative scatter in the data. Further analysis is performed as if there were no intensity dependence at all.

Marling and Herman's multimode dissociation data[36] were employed for our analysis of the dissociation yield. It was performed using the static-cell technique. Figure 14 plots the data which are consistent with the thermal curve, within experimental error.

We now consider a somewhat larger molecule, C_3F_7I, a completely substituted propane. Its strong absorption feature is nearest to the CO_2 laser line at 1041.28 cm^{-1}. The C_3F_7I absorption data are shown in Fig. 15. All of the data from each of the three pulse types fall on the same line, showing that the laser radiation is absorbed equally well in each case, at constant fluences. No discernible intensity effect is observed. This is in striking contrast to the smaller molecules and completes the progression we have observed. One would expect no effect of intensity upon the dissociation yield. This is indeed what we have experimentally observed. The dissociation data are plotted in Fig. 16. Again, there is agreement with the thermal curve.

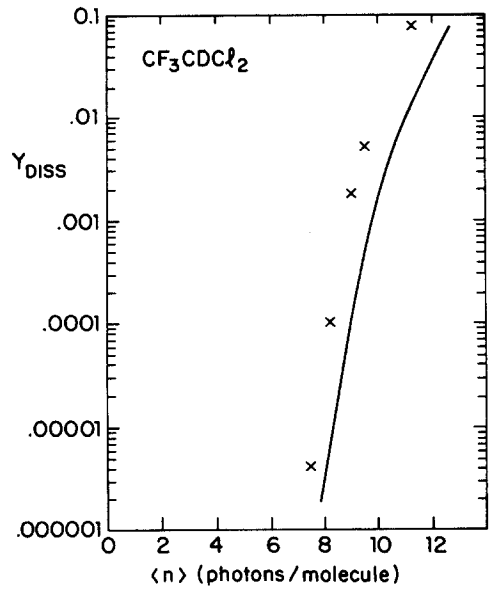

FIG. 14. Semilog plot of the dissociation yield Y_{diss} as a function of the average number of photons absorbed per molecule in CF_3CDCl_2. The dissociation data from Ref. 40 is compared with our optoacoustic data. Also shown is the yield assuming a thermal distribution at an energy corresponding to $\langle n \rangle$.

Hexafluoracetone (HFA), a ten-atom molecule has a strong absorption feature centered near the CO_2 laser line at 971.9 cm^{-1}. Figure 17 shows the absorption data. There is absolutely *no* detectable intensity dependence for absorption in HFA.

The main absorption feature of HFA is rather broad. Figure 18 compares the multiphoton energy deposition in HFA excited at two frequencies of the CO_2 laser, 971.9 and 944.2 cm^{-1}. The upper trace is copied from Fig. 17 and the lower trace contains data from three laser pulse types superimposed. Note that even when we are almost 30 cm^{-1} away from HFA's line center, there is still strictly fluence dependent absorption. The detuning does not lead to discrete state

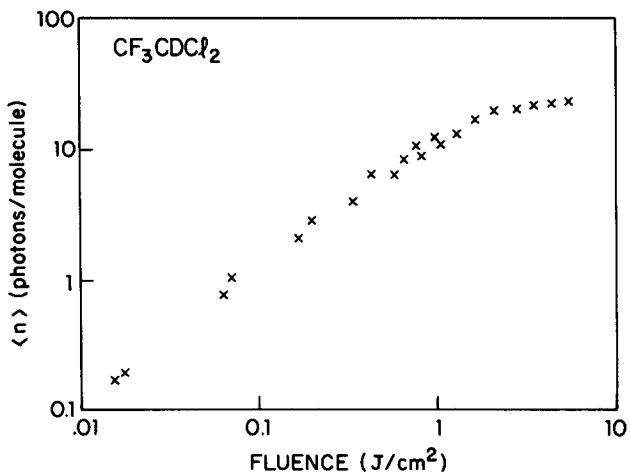

FIG. 13. Log–log plot of the average number of photons absorbed per molecule $\langle n \rangle$ as a function of CO_2 laser fluence at 937 cm^{-1} in CF_3CDCl_2. The data points are the same for 100 ns single and multimode pulses, as well as for 0.5 ns pulses.

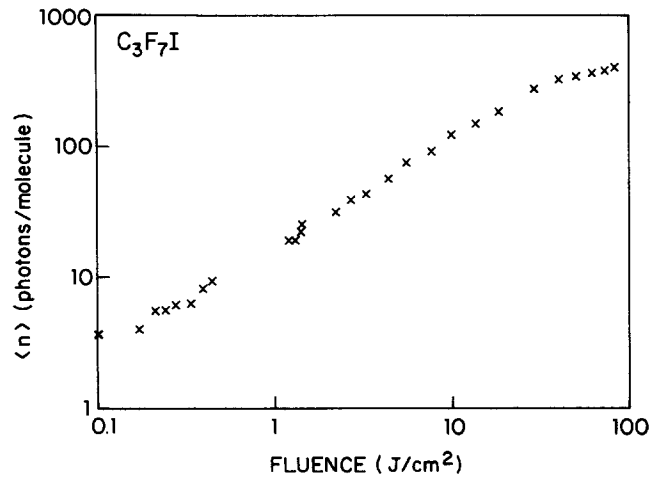

FIG. 15. Log–log plot of the average number of photons absorbed per molecule $\langle n \rangle$ in C_3F_7I as a function of laser fluence at 1041 cm^{-1}. The data points are superimposed for three different pulse types, 100 ns single and multimode and 0.5 ns.

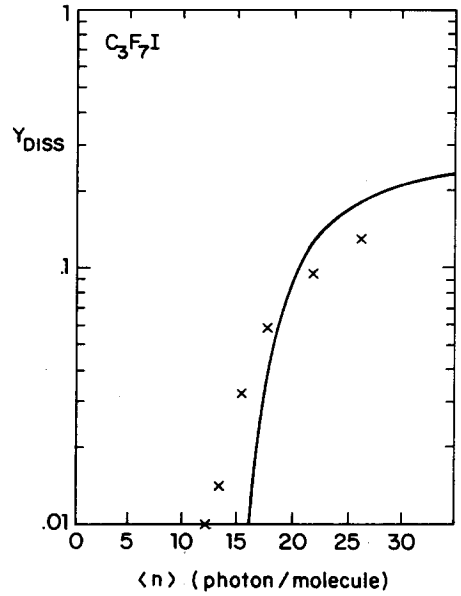

FIG. 16. Semilog plot of the dissociation yield Y_{diss} as a function of the average number of photons absorbed per molecule in C_3F_7I. There is no difference between the 100 ns and 0.5 ns data. The solid curve is the yield calculated on the assumption of a thermal distribution at an energy corresponding to $\langle n \rangle$.

effects but only to decreased quasicontinuum absorption probabilities.

At the lower fluences, the absorption at the higher frequency is roughly 20 times as high as that at the lower frequency. This difference diminishes greatly at the high-fluence end of the graph. The convergence of the two sets of data indicates that the infrared absorption feature is broadening and red shifting as the molecule absorbs energy. Similar behavior occurs upon heating as has been shown, for example, in SF_6.[37] Between 1–10 J/cm^2 the data indicate a decreasing differential cross section for 972 cm^{-1} excitation and an increasing differential cross section for 944 cm^{-1} excitation. This point also emphasizes the fact that absorption features persist in the quasicontinuum. A flat infrared absorption spectrum is not expected. Broad absorption features, > 10 cm^{-1}, give an indication of the time scale where one might expect that Fermi's Golden Rule will not apply, however, they are consistent with a statistical coupling of vibrational modes and a rate equation analysis given the laser pulse durations and intensities necessary for the excitation of the larger polyatomics in this study.

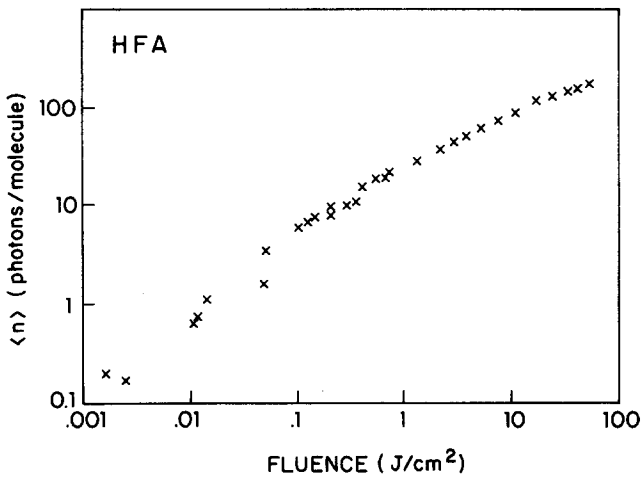

FIG. 17. Log–log plot of the average number of photons absorbed per molecule $\langle n \rangle$ in hexafluoroacetone (HFA), as a function of laser fluence at 972 cm^{-1}. The data points are superimposed for three different pulse types, 100 ns single and multimode and 0.5 ns.

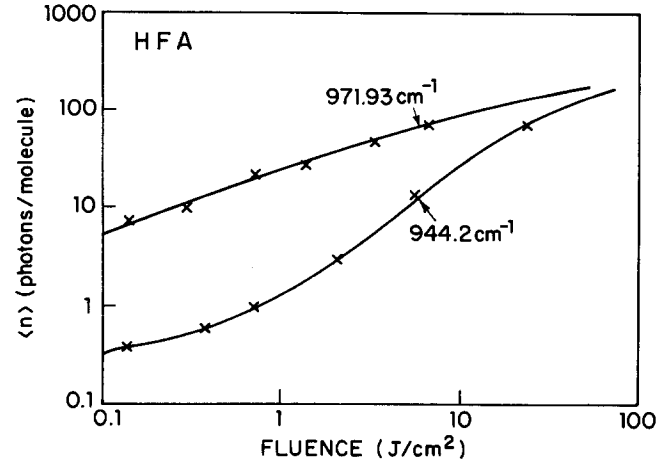

FIG. 18. Log–log plot comparing the optoacoustic signals in hexafluoroacetone at 972 and 944 cm^{-1}. In neither case is there any pulse duration dependence to the data.

The dissociation yield for hexafluoroacetone as a function of fluence has been obtained by Fuss *et al.*[38] For completeness their data are replotted in Fig. 19 vs $\langle n \rangle$, which was obtained by us as a function of fluence. As with other large molecules, the data are consistent with the thermal curve. There is no intensity dependence in the dissociation yield in

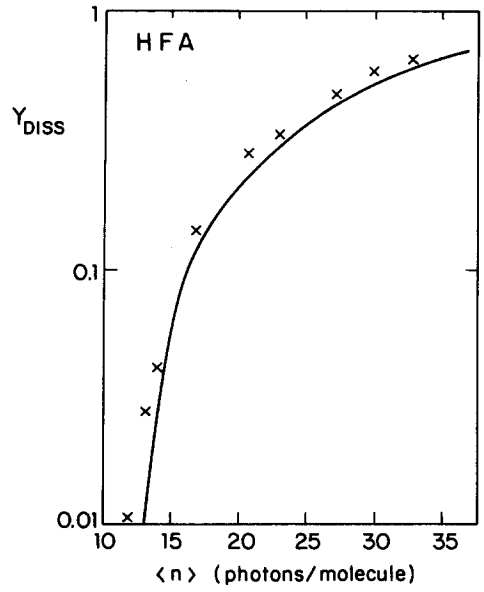

FIG. 19. Semilog plot of the dissociation yield Y_{diss} as a function of the average number of photons absorbed per molecule in hexafluoroacetone. There is no difference between the 100 and 0.5 ns data. The solid curve is calculated on the assumption of a thermal distribution at an energy corresponding to $\langle N \rangle$.

hexafluoroacetone which has a density of states five orders of magnitude higher than SF_6 at 12 photons of internal excitation.[39]

IV. DISCUSSION

The trends we have observed in the behavior of collisionless IRMPE and IRMPD are summarized in Table I. No collisionless dissociation by monochromatic IR radiation has been reported for diatomic molecules. There is only one ladder of discrete states for a single anharmonic oscillator mode. Theoretical calculations for HF show that a true multiphoton dissociation process could only become observable at intensity levels exceeding 10^{13} W/cm^2.[40] At these levels ionization processes would mask pure IRMPD. Therefore, the absence of experimental results for collisionless dissociation is understandable.

For triatomic and four-atom molecules the limiting factor in IRMPE is the true multiphoton process from the initial ground state with energy E_g, to a state with an energy in the range $E_g = nh\nu_L + nh\Delta\nu_L$ required by energy conservation. If such a state exists and the energy mismatches through a ladder of intermediate states are not too large in comparison to the Rabi frequency, the highly excited state may be reached with a probability which rapidly increases with laser power. This excitation mechanism through the discrete state region is power limited. At the end of the laser pulse most of the molecules have returned to their initial state. They represent the large bottlenecked fraction characteristic of a very sparse energy level diagram. Even though admixtures of intermediate states during the laser pulse may be substantial, energy conservation considerations prevent the molecules from remaining in the detuned discrete levels after the pules.

A small fraction of the small molecules reaches highly excited molecular eigenstates. The wave functions in this regime are superpositions of all normal mode functions due to large anharmonic and Coriolis couplings. In this regime further excitation proceeds by a succession of low order multiphoton or even the single photon processes describable by the rate equation description of quasicontinuum excitation. The IRMPD yield is comparable to the total yield of excited molecules. The stepwise cross sections in NO_2 double resonance experiments[27] show the relative ease of excitation through these excited states as does the distribution of excited molecules[7] in DN_3 and SO_2.

As one progresses to larger molecules, the quasicontinuum gradually reaches down to lower excitation energies, and, for the largest, heaviest species studied here, most molecules in a thermal ensemble at room temperature are already in the quasicontinuum. Thus a gradual transition to a fluence dominated dependence of IRMPE and IRMPD occurs, and the bottlenecked fraction gradually approaches zero. The bottlenecking effect leads to a bimodal ("hot" and "cold") distribution which has been studied extensively by workers in the Soviet Union.[1(c)]

There is no *a priori* reason to expect that IRMPE in the quasicontinuum will lead to a thermal distribution. The actual distribution will be determined by the dynamics of the rate equations. Published numerical models [1(b),41] of rate equation excitation do not give a Boltzmann distribution but neither do they give a mean energy and high energy tail consistent with our measurements. It is certainly intriguing that the excitation of molecules free of bottlenecking effects leads to a final mean energy and high energy tail *consistent* with a thermal distribution. There are no adjustable parameters in the thermal model. At the very least it is extremely strong evidence that in the highly excited levels of the quasicontinuum there is an equipartitioning of energy over all normal mode vibrations.

TABLE I. A summary of experimental results on the infrared multiphoton excitation of polyatomic molecules having a vibrational feature resonant with CO_2 laser transitions. Effects of region with discrete states dominate in small molecules while quasicontinuum effects dominate in larger ones.

Discrete Region of Molecular Eigenstates	Quasicontinuum
Excitation via resonantly enhanced multiphoton steps	Stepwise, incoherent excitation
Little population of excited states due to lack of resonances	Broad distribution of final excited states

Diatomics	3 and 4 atom molecules	4-6 atom molecules	6-10 atom molecules	10+ atom molecules
Strict multiphoton excitation	Intensity controls excitation	Both intensity and fluence important	Fluence dominates intensity	Fluence controls excitation
No known examples of IR dissociation	At 100 GW/cm^2: -small diss. yield -small <n>	Unity dissociation yield, 10-50 J/cm^2 lower for < 1 ns t_p	Unity dissociation yield, 10 J/cm^2	Unity dissociation yield, 1-10 J/cm^2
		Large bottleneck	Small bottleneck	No bottleneck
Theoretical calc. 10-100 TW/cm^2 for dissociation	Discrete region dominates	Both discrete states and quasicontinuum effects	Quasicontinuum dominates	Molecule starts in quasicontinuum

It appears that a large body of work by other groups is also consistent with the noted general trends. We shall briefly mention some other work on the same molecules studied in this report. The most studied molecule in the field is SF_6. Optoacoustic measurements are in essential agreement with results presented here.[42] A molecular beam study has shown that the dissociation product energies are consistent with a statistical partitioning of the energy.[43] Apatin *et al.*[34] have shown that all initially populated rotational levels participate in the excitation at fluences below 0.1 J/cm^2, intensities below 10^6 W/cm^2, indicating the dominant role of multiphoton transitions over the discrete levels. Raman studies of SF_6 molecules following IRMPE show two distinct ensembles, hot and cold molecules.[44] This is further evidence that population of excited states is unlikely until the density of states ensures stepwise resonances. Recently, the two ensemble distinction has been shown to extend down to fluences as low as 10^{-2} J/cm^2.[45] Mazur *et al.* also reported results indicating a thermal distribution of molecules excited to the quasicontinuum, in agreement with our results.[45] Similarly, in CF_3I, a corroborating series of optoacoustic,[46] dissociation product,[47] and Raman[44] measurements have been performed. An extensive energy deposition and dissociation yield study on CF_3I has been reported by Bagratashvili *et al.*[48] Their results are consistent with ours and they point out the importance of the bottleneck fraction. Finally, Stephenson, King, and co-workers have performed extensive experiments on CF_2HCl, CF_2CFCl, and similar molecules which show intensity effects in the excitation but a statistical distribution of dissociation products.[24,25,49] For further work, the reader is referred to the reviews.[1]

We must point out that there are a few experimental results of IRMPE that are at variance with the excitation mechanism presented here. We have commented on previously reported OCS experiments[50] elsewhere.[3] Recent experiments on OCS are in agreement with our work.[51] Results on Cl_2CS are totally inconsistent.[52] The ground level of this molecule is depopulated at intensities much lower than the small molecules we have studied. A recent study of SF_6 yields results which are consistent, we believe, with our description of IRMPE but which have been interpreted quite differently.[53] The SF_6 was excited by pulses of similar duration but widely differing bandwidths. The wider bandwidth pulses gave increased IRMPE in a manner similar to the effects we observe when using multimode 100 ns pulses instead of single mode. The authors of Ref. 53 interpreted these results as evidence of a lack of any quasicontinuum in SF_6 at energies up to ten absorbed IR photons. However, the discrete state region can easily be the rate limiting step in IRMPE for the narrow bandwidth pulses. The increased IRMPE efficiency with the wide bandwidth pulses is due to the onset of the quasicontinuum at lower excitation energies. Therefore, these new results show that discrete state effects are playing a role in SF_6 excitation but the experiment does not give an unambiguous estimate of the excitation energy necessary for the quasicontinuum. Also consistent is recent work with SF_6 excited by intense picosecond pulses which shows the breakdown of fluence dependent excitation for sufficiently rapid excitation rates.[54] These experiments were conducted in a regime where inequality (3) is not expected to be satisfied and coherent excitation again plays a role in the excitation through the quasicontinuum.

We have made no effort to probe the details of how molecular selection rules are broken in the transition from region one to quasicontinuum excitation. There must be a transition regime between the unmixed, sparse accessible state region and the totally mixed quasicontinuum. A recent set of experiments on jet cooled anthracene indicates a transition from unmixed discrete states at excitation energy up to 1000 cm^{-1} to complete mixing at 1800 cm^{-1} in this large molecule.[55] In the intermediate range mixing is incomplete and quantum beats are observed.[55] The density of vibrational states is greater than 100 per cm^{-1} in the intermediate range. In contrast, NO_2 near the dissociation threshold appears to be totally mixed at a density of vibrational states of less than 1 per cm^{-1}.[27] Therefore, the density of vibrational states is, by itself, not a good measure of the onset of the mixing. However, our results indicate that the mixing, once begun, rapidly leads to a statistical coupling of the vibrational modes as the excitation energy is increased.

The breakdown of rotational selection rules can greatly increase the density of states accessible to IR excitation. From double resonance experiments on NO_2, a density of accessible states more than two orders of magnitude larger than the Whitten–Rabinovitch calculation of the vibrational state density is indicated.[27] If this is a general phenomenon it would further explain the efficiency of IR pumping in highly excited vibrational states of small molecules. This factor pushes the density of accessible states above the quasicontinuum threshold for the small molecules to near or just below the dissociation limit. In larger polyatomics the effects of rotations in IRMPE are seen in supersonic molecular beam experiments where the rotational temperature of the molecule is reduced to a few degrees Kelvin. Some decrease of the IRMPE absorption feature in SF_6 is measured, consistent with an increase in the number of photon necessary to reach the quasicontinuum.[21,35] The influence of any breakdown of rotational selection rules in the excitation of larger molecules is probably overshadowed by the rapid increase in the density of vibrational states.

In conclusion, the general trends in Table I describe the behavior of most molecules subjected to intense quasimonochromatic near-resonant IR radiation. We emphasize again that the laser intensity and frequency spectrum, as well as the molecular characteristics, are integral factors in determining the definition and relative importance of the discrete state and quasicontinuum excitation regimes. The details of individual molecular energy eigenstates are obscured by the many states, initial, intermediate, and final, that participate in the IRMPE of polyatomic molecules. It is only when the quasicontinuum region dominates the excitation that it is possible for a large fraction of the molecular ensemble to be excited under realizable conditions of IR laser fluence and intensity.

ACKNOWLEDGMENTS

This research was supported by the U.S. Army Research Office under contract No. DAAG29-81-K-0071, and

the Joint Services Electronics Program of the U.S. Department of Defense under Contract No. N00014-84-K-0465.

[1]For recent reviews see, for example: (a) W. Fuss and K. L. Kompa, Prog. Quantum Electron. **7**, 117 (1981); (b) D. S. King, in *Dynamics of the Excited State*, edited by K. P. Lawley (Wiley, New York, 1982);(c) V. S.Letokhov, *Nonlinear Laser Chemistry* (Springer, New York, 1982).
[2]N. Bloembergen and E. Yablonovitch, Phys. Today **31**, (5) 23 (1978).
[3]T. B. Simpson and N. Bloembergen, Opt. Commun. **37**, 256 (1981).
[4]T. B. Simpson and N. Bloembergen, Chem. Phys. Lett. **100**, 325 (1983).
[5]J. G. Black, Ph.D. thesis, Harvard University, 1980 (unpublished).
[6]J. G. Black, P. R. Kolodner, M. J. Shultz, E. Yablonovitch, and N. Bloembergen, Phys. Rev. A **19**, 704 (1979).
[7]T. B. Simpson, E. Mazur, K. K. Lehmann, I. Burak, and N. Bloembergen, J. Chem. Phys. **79**, 3373 (1983).
[8]N. Bloembergen, I. Burak, and T. B. Simpson, J. Mol. Struct. **113**, 69 (1984).
[9]S. Mukamel and J. Jortner, J. Chem. Phys. **65**, 5204 (1976).
[10]J. R. Ackerhalt and J. H. Eberly, Phys. Rev. A **14**, 1750 (1976).
[11]B. Carmeli and A. Nitzan, J. Chem. Phys. **70**, 3016 (1979).
[12]I. Schek and J. Jortner, J. Chem. Phys. **70**, 3016 (1979).
[13]P. J. Robinson and K. A. Holbrook, *Unimolecular Reactions* (Wiley, New York, 1973).
[14]J. Stone, E. Thiele, and M. F. Goodman, Chem. Phys. Lett. **71**, 171 (1980).
[15]J. Stone, E. Thiele, and M. F. Goodman, J. Chem. Phys. **71**, 1712 (1981).
[16]H. S. Kwok and E. Yablonovitch, Rev. Sci. Instrum. **46**, 814 (1975).
[17]J. G. Black, Rev. Sci. Instrum. **51**, 655 (1980).
[18]D. Tal, V. P. Oppenheim, G. Koren, and M. Okon, Chem. Phys. Lett. **48**, 67 (1977).
[19]J. D. Lambert, *Vibrational and Rotational Relaxation in Gases* (Clarendon, Oxford, 1977).
[20]R. C. Sharp, E. Yablonovitch, and N. Bloembergen, J. Chem. Phys. **74**, 5357 (1981).
[21]D. Bassi, A. Borschetti, G. Scoles, M. Scotoni, and M. Zen, Chem. Phys. **71**, 239 (1982).
[22]M. J. Shultz and E. Yablonovitch, J. Chem. Phys. **68**, 3007 (1978).
[23]V. N. Donnelly, D. G. Keil, and F. Kaufmann, J. Chem. Phys. **71**, 659 (1979).
[24]C. J. Halstead and B. A. Thrush, Proc. R. Soc. London Ser. A **295**, 363 (1966).
[25]R. D. Shelton, A. H. Nielson, and W. H. Fletcher, J. Chem. Phys. **21**, 2178 (1953).
[26]S. Kimel, D. Feldmann, J. Laukemper, and K. H. Welge, J. Chem. Phys. **76**, 4893 (1982).
[27]J. Y. Tsao, T. B. Simpson, N. Bloembergen, and I. Burak, J. Chem. Phys. **77**, 1274 (1982).
[28]Ph. Avouris, M. M. T. Loy, and I. Y. Chan, Chem. Phys. Lett. **63**, 624 (1979).
[29]T. B. Simpson, Ph.D. thesis, Harvard University, 1983.
[30]D. S. King and J. C. Stephenson, Chem. Phys. Lett. **66**, 33 (1979).
[31]J. C. Stephenson and D. S. King, J. Chem. Phys. **78**, 1867 (1983).
[32]M. Rossi, J. R. Barker, and D. M. Golden, Chem. Phys. Lett. **65**, 523 (1979).
[33]D. R. Stull and H. Prophet, *JANAF Thermochemical Tables*. 2nd ed. Natl. Bur. Stand. (U.S. GPO, Washington, D. C., 1971).
[34]V. M. Apatin, V. M. Krivtsun, Yu. A. Kuritsyn, G. N. Makarov, I. Pak, I. I. Zasavitskii, and A. P. Shotov, JETP Lett. **37**, 431 (1983).
[35]A. Boschetti, M. Zen, D. Bassi, and M. Scotoni, Chem. Phys. **87**, 131 (1984).
[36]J. B. Marling and I. P. Herman, Appl. Phys. Lett. **34**, 439 (1979).
[37]A. V. Nowak and J. L. Lyman, J. Quant. Spectrosc. Radiat. Transfer **15**, 945 (1975).
[38]W. Fuss, K. L. Kompa, and F. M. G. Tablas, Faraday Discuss. **67**, 180 (1979).
[39]J. L. Lyman, G. P. Quigley, and O. P. Judd, in *Single-Infrared Frequency Studies of Multiple-Photon Excitation and Dissociation of Polyatomic Molecules*, edited by C. Cantrell (Springer, Heidelberg, 1980).
[40]D. W. Noid and J. R. Stine, Chem. Phys. Lett. **65**, 153 (1979).
[41]E. R. Grant, P. A. Schultz, As. S. Sudbo, Y. R. Shen, and Y. T. Lee, Phys. Rev. Lett. **40**, 115 (1978).
[42]G. Hancock and A. J. Macrobert, Chem. Phys. Lett. **100**, 312 (1983).
[43]P. A. Schultz, Aa. S. Sudbo, E. R. Grant, Y. R. Shen, and Y. T. Lee, J. Chem. Phys. **71**, 239 (1982).
[44]V. N. Bagratashvili, Yu. G. Vinier, V. S. Dolzhikov, S. F. Kol'yakov, V. S. Letokhov, A. A. Makarov, L. P. Malyavkin, E. A. Ryabov, E. G. Sil'kis, and V. D. Titov, Sov. Phys. JETP **53**, 512 (1981).
[45]E. Mazur, I. Burak, and N. Bloembergen, Chem. Phys. Lett. **105**, 258 (1984).
[46]J. M. Weulersse and R. Genier, Appl. Phys. **24**, 363 (1981).
[47]Aa. S. Sudbo, P. A. Schultz, E. R. Grant, Y. R. Shen, and Y. T. Lee, J. Chem. Phys. **70**, 912 (1979).
[48]V. N. Bagratashvili, V. S. Dolzhikov, V. S. Letokhov, A. A. Makarov, E. A. Ryanbov, and V. V. Tyakht, Sov. Phys. JETP **50**, 1075 (1979).
[49]J. C. Stephenson, S. E. Bialkowski, D. S. King, E. Thiele, J. Stone, and M. F. Goodman, J. Chem. Phys. **74**, 3905 (1981).
[50]D. Proch and H. Schroeder, Chem. Phys. Lett. **61**, 426 (1979).
[51]A. Schwebel and A. M. Ronn, J. Phys. Chem. **87**, 4375 (1983).
[52]D. M. Brenner, N. N. Spencer, and J. I. Steinfeld, J. Chem. Phys. **78**, 136 (1983).
[53]S. S. Alimpiev, W. Fuss, K. L. Kompa, C. Schwab, and Wan Chong-Yi, Appl. Phys. B **35**, 1 (1984).
[54]P. Mukherjee and H. S. Kwok, Chem. Phys. Lett. **111**, 33 (1984); H. S. Kwok, E. Yablonovitch, and N. Bloembergen, Phys. Rev. A **23**, 3094 (1981).
[55]W. R. Lambert, P. M. Felker, and A. H. Zewail, J. Chem. Phys. **81**, 2209, 2217 (1984).